

Automatic Approach for Classifying Sympathetic Quasiperiodic, n:m Periodic and Aperiodic Dynamics Produced by Lung Inflation in Rats

A Porta¹, N Montano², R Furlan², C Cogliati², S Guzzetti², A Malliani², H-S Chang³,
K Staras³, MP Gilbey³

¹DiSP LITA di Vialba, Università degli Studi di Milano, Milan, Italy

²DiSC, Università degli Studi di Milano, Medicina Interna II, Milan, Italy

³Department of Physiology, University College London, London, UK

Abstract

A method for classifying non linear interactions between two event series, a forcing input and a forced output, is proposed. The approach allows to classify: 1) independent dynamics; 2) quasiperiodic dynamics; 3) n:m periodic synchronized dynamics in which n events of the forced signal occur every m cycles of the driving signal; 4) aperiodic dynamic. The method is automatic and fully independent of the researcher's judgment. In addition, it calculates the ratio and the strength of the coupling in the case of synchronized dynamics. The method is applied to verify whether sympathetic oscillators underlying the discharges of single postganglionic sympathetic neurons innervating the ventral caudal artery of the rat tail could be synchronized by the lung inflation cycle. The application confirms the capability of the method in classifying the dynamics and the synchronizing action of the lung inflation cycle over the single sympathetic neuron discharges.

1. Introduction

Perturbing the activity of biological oscillators by means of a periodical driving input results in full independent, quasiperiodic, n:m phase-locked or aperiodic dynamics depending on detuning (i.e. the difference between the frequencies of the forcing input and of autonomous self-sustained oscillator), on the amplitude of the driving input and on the strength of the coupling between the two oscillators [1]. Usually classification of these dynamics is obtained by superimposing the forced and forcing signals [2]. This practice leads to a classification largely dependent of the experience of the researcher and not fully reproducible. Moreover, it becomes difficult to perform when sliding dynamics or relative co-ordinations produce changes of the coupling ratio. Also noise corrupting the repetitive coupling scheme may render impossible a robust classification based on visual inspection. In addition, the

strength of the coupling between driving and driven oscillators cannot be quantified.

The aim of this study is to propose an automatic, fully reproducible, method for classifying non linear interferences between forcing and forced event series [3]. Four types of dynamics are classified: 1) independent dynamics in which the relative phase grows uniformly; 2) quasiperiodic dynamics in which the relative phase grows non-uniformly; 3) n:m synchronization in which the two event series are phase-locked such a way that n events of the forced activity occurred in m cycles of the forcing signal; 4) aperiodic dynamics in which the relative phase changes irregularly. The method is based on the contemporaneous use of several tools (the relative phase probability density function, the probability density function of the count of the forced responses per forcing cycle, the normalized corrected conditional entropy of the relative phase sequence and a surrogate data approach).

The method was applied to data extracted from one anesthetized, artificially ventilated rat to evaluate the interactions between the lung inflation cycle and two different sympathetic oscillators monitored through the discharges of two, simultaneously recorded, single postganglionic sympathetic neurons innervating the ventral caudal artery in the rat tail [4] as a function of the mechanical ventilatory rate.

2. Methods

2.1. Tools for classifying interactions

Given two event series $t_u = \{t_u(k), k=1, \dots, K\}$ and $t_y = \{t_y(j), j=1, \dots, J\}$, where $t_u(k)$ and $t_y(j)$ represent the times of occurrence of the k-th and j-th forcing and forced events of u and y respectively, the relative phase of the j-th event of y with respect to u is defined as

$$\varphi(j) = \frac{2\pi(t_y(j) - t_u(k))}{t_u(k+1) - t_u(k)}$$

with $t_u(k) \leq t_y(j) \leq t_u(k+1)$ and where $t_u(k+1) - t_u(k)$ is the duration of the k-th forcing cycle. When no driven response is found in a forcing cycle, the relative phase is

set to -1 , thus codifying a missed response of y . Therefore, the relative phase series $\varphi = \{\varphi(i), i=1, \dots, J+L\}$ is a mixed sequence of J values ranging from 0 to 2π and L values equal to -1 . The relative phase series is referred to as phase in the following.

The first tool on which classification is based is the phase probability density function (PPDF). It is estimated with a phase resolution of 0.25 radians after suppression of the values codifying the missed responses (i.e. -1). The parameters extracted from PPDF are: 1) the Shannon entropy (SE) of the PPDF; 2) the number of peaks. SE ranges from 0 in case of a PPDF with a unique peak with probability 1 to a theoretical maximum value equal to 3.22 in case of a uniform PPDF (with that specific phase resolution and using the natural logarithm to calculate SE). The presence of peaks in the PPDF is taken as an indication of the repetitive occurrence of events of y at specific phases of u . The second tool used to decide the class to which the non linear interferences belong is the probability density function of the number x of forced responses of y per forcing cycle of u (i.e. the count probability density function, CPDF). The parameter extracted from the CPDF is the mean value $\text{av}[x]$. Therefore, $1/\text{av}[x]$ provides the mean number of forcing cycles necessary to count one response of y . The third tool is the normalized corrected conditional entropy [5] (NCCE), a function based on the conditional entropy but capable of preventing its artificial decrease related to the shortness of the data sequence. This function is applied to the phase sequence after normalization (i.e. the mean value is subtracted and the result is divided by the standard deviation) and quantization. Normalization is applied only to values different from -1 (i.e. it is not applied to the missed responses). After normalization the normalized sequence is uniformly spread on 6 quantization values (from 0 to 5). As the value -1 again continues to codify the missed responses even after quantization, the actual number of quantization levels are 7 . From the NCCE a regularity index ρ was derived [5]. This index ranges from 0 (completely unpredictable phase series) to 1 (fully predictable phase series).

2.2. Surrogate data approach

Classification is based on a surrogate data approach [6] applied to the phase series. Two surrogate data sets are generated. The first set consists of 20 realizations of identically distributed white noise ranging from 0 to 2π . This set is useful to test whether the PPDF is uniform. Indeed, if the SE calculated on the original phase series (SE_o) is smaller than a SE significance threshold derived from the surrogate data set (i.e. $\text{av}[SE_s] - 2 \cdot \text{sd}[SE_s]$, where av and sd are the mean and standard deviation operators applied to the Shannon entropies calculated on surrogate phase realizations, SE_s), then the null hypothesis of a flat PPDF is rejected. In the case that the $SE_o < \text{av}[SE_s] -$

$2 \cdot \text{sd}[SE_s]$, the number of PPDF peaks is searched as follows. The $PPDF_o$ is compared to a significance threshold derived from $PPDF_s$. At a given phase if the $PPDF_o$ is larger than $\text{av}[PPDF_s] + 2 \cdot \text{sd}[PPDF_s]$, then that specific phase is more likely than the same phase in a uniform distribution. If this excess is larger than 0.03 and takes place for an isolated phase, then one reliable peak is detected. If this excess is larger than 0.03 and it takes place for several adjacent phases, then the number of reliable peaks is equal to the number of relative maxima. If, at any given phase, $PPDF_o$ is below the PPDF significance threshold or the excess is below 0.03 no reliable peak is detected.

The second set of surrogate data consists of 20 realizations of processes obtained by shuffling the temporal order of the samples of the phase series (including the values codifying the missing responses) and of the number of driven events per driving cycle, thus destroying correlation between samples but maintaining the PPDF and CPDF. Two independent random permutations are utilized. This set is useful to test whether the phase sequence is unpredictable. Indeed, if the regularity index ρ calculated on the original phase series (ρ_o) is larger than a ρ significance threshold derived from the surrogate data set (i.e. $\text{av}[\rho_s] + 2 \cdot \text{sd}[\rho_s]$, where ρ_s are the regularity indexes calculated on the surrogate phase series), then the null hypothesis of a unpredictable phase series is rejected.

2.3. Classification

The interactions between u and y event series are classified according to three tests: 1) SE test; 2) PPDF test; 3) ρ test. The SE test checks if $SE_o < \text{av}[SE_s] - 2 \cdot \text{sd}[SE_s]$. The PPDF test finds out the number of reliable peaks in the $PPDF_o$. The ρ test checks if $\rho_o > \text{av}[\rho_s] + 2 \cdot \text{sd}[\rho_s]$. If the SE test is not passed and the ρ test is fulfilled, then u and y are uncoupled. If both SE and ρ tests are passed but the PPDF test does not reveal any reliable peak, then u and y are quasiperiodic. If both SE and ρ tests are passed and the PPDF test finds out some reliable peaks, then u and y are periodic. If the ρ test is not fulfilled, then u and y are aperiodic. In the case of periodic dynamics: 1) the numerator n and the denominator m of the coupling ratio are estimated as the number of reliable peaks in $PPDF_o$ and as the rounding to the nearest integer of the product between n and $1/\text{av}[x]$ respectively; 2) ρ_o is taken as a measure of the coupling strength.

3. Experimental protocol and data analysis

We make reference to [4] for a complete description of the experimental preparation. Briefly, one male Sprague Dawley rat was anesthetized and artificially ventilated.

Tracheal pressure was recorded and the times of occurrence of the lung inflation onset (LIO) were extracted, thus forming the event series $t_{LIO}=\{t_{LIO}(k), k=1,\dots,N_{LIO}\}$ where $t_{LIO}(k)$ was the timing of the k -th LIO and $N_{LIO}-1$ is the total number of ventilatory cycles. Using a focal technique the discharges of two single postganglionic neurons (PGNs) were simultaneously recorded from the surface of the ventral caudal artery in the tail. The temporal position of the PGN action potential peak (PGNAPs) was detected, thus forming the two event series $t_{PGNAP1}=\{t_{PGNAP1}(j), j=1,\dots,N_{PGNAP1}\}$ and $t_{PGNAP2}=\{t_{PGNAP2}(j), j=1,\dots,N_{PGNAP2}\}$, where $t_{PGNAP1}(j)$ and $t_{PGNAP2}(j)$ represented the timing of the j -th PGNAP and N_{PGNAP1} and N_{PGNAP2} were the total number of PGNAPs.

Five lung inflation rates were utilized to perturb the activity of the sympathetic oscillators (0.58, 0.64, 0.76, 0.95, 1.99 Hz). Four of these frequencies were in the range of the dominant intrinsic rhythm of the PGN

discharge (from 0.4 to 1.2 Hz), while the remaining one (i.e. 1.99 Hz) was largely above this range [4]. Experiments were carried out under central apnea as verified from by the absence of diaphragm EMG activity. PH, PaO₂ and PaCO₂ were continuously monitored and maintained in normal range.

4. Results

Fig.1a shows an example of LIO and PGNAP event series (solid and dotted lines). PGNAPs occur more likely at one specific phase of the lung inflation cycle. PPDF_o (Fig.1b, filled bars) is different from a uniform distribution. Indeed, $SE_o=2.37$ is smaller than SE significance threshold (i.e. 3.16) and one dominant peak emerging from the PPDF significance threshold (Fig.1b, open bars) can be detected, thus leading to $n=1$. Fig.1c proves that $av[x]$ is larger than 1 (i.e. 1.41), thus leading to $m=1$. NCCE_o (Fig.1d, solid line) shows a deep

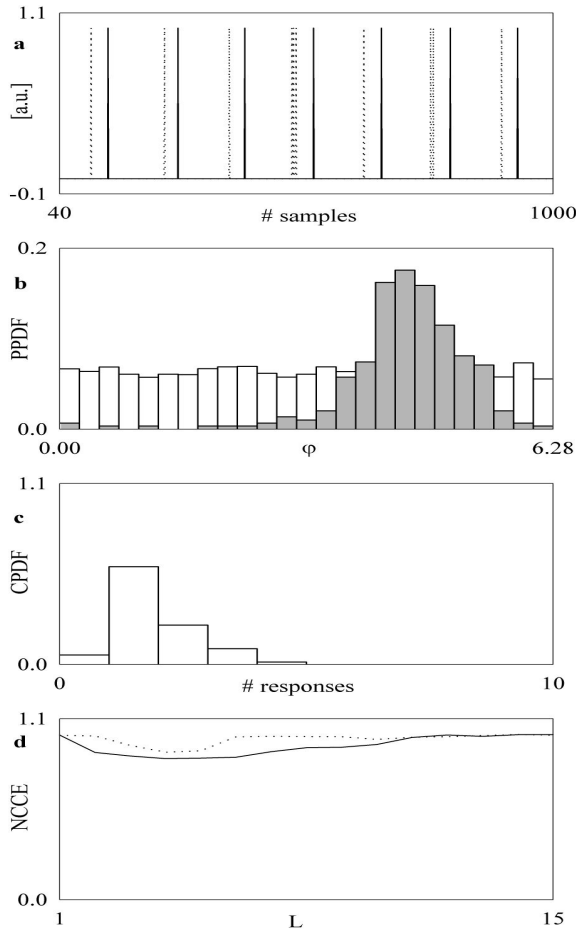


Figure 1. 1:1 synchronization: LIO (a, solid line) and PGNAP (a, dotted line) event series, PPDF_o (b, filled bars) and PPDF significance threshold (b, open bars), CPDF (c) and NCCE calculated on the original phase series (d, solid line) and on a realization of surrogate data (d, dotted line). See text.

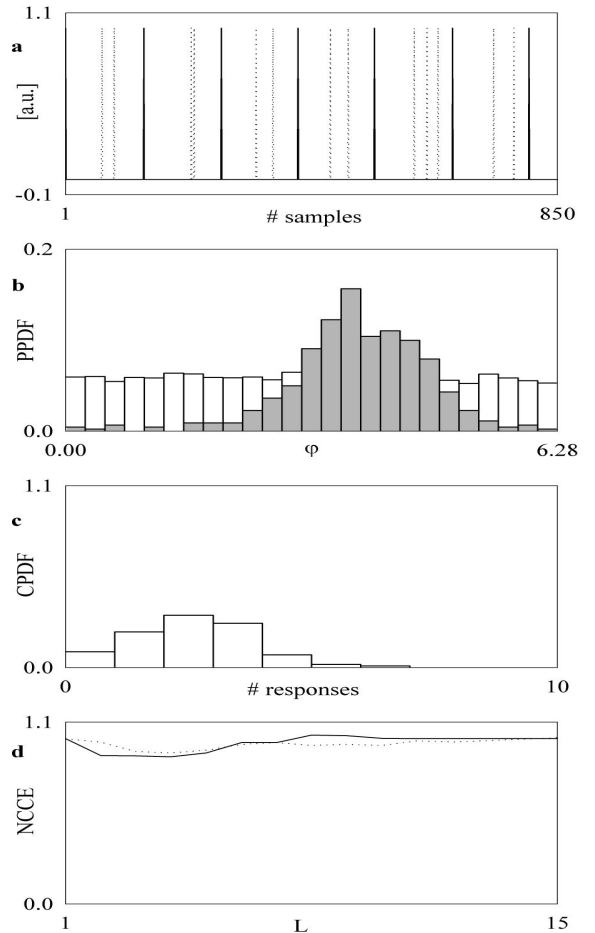


Figure 2. 2:1 synchronization: LIO (a, solid line) and PGNAP (a, dotted line) event series, PPDF_o (b, filled bars) and PPDF significance threshold (b, open bars), CPDF (c) and NCCE calculated on the original phase series (d, solid line) and on a realization of surrogate data (d, dotted line). See text.

minimum, thus producing a $\rho_0=0.14$ above the ρ significance threshold (i.e. 0.11). From all these data the dynamics is classified as 1:1 synchronized.

Fig.2a shows another example of LIO and PGNAP event series (solid and dotted lines). PGNAPs occur more likely at two specific (even though very close) phases of the lung inflation cycle. PPDF₀ (Fig.2b, filled bars) is different from a uniform distribution. Indeed, $SE_0=2.59$ is smaller than SE significance threshold (i.e. 3.18) and a dominant peak with two relative maxima emerging from the PPDF significance threshold (Fig.2b, open bars) can be detected, thus leading to $n=2$. Fig.2c proves that $av[x]$ is larger than 2 (i.e. 2.11), thus leading to $m=1$. NCCE₀ (Fig.2d, solid line) shows a minimum (although not deep), thus producing a $\rho_0=0.11$ slightly above the ρ significance threshold (i.e. 0.10). From all these data the dynamics is classified as 2:1 synchronized.

While varying the lung inflation rate, we found 6 examples of periodic dynamics (60%, one case of 1:1, 2:2, 3:2, 2:5 and two cases of 2:1 periodic patterns) and 4 examples of aperiodic dynamics (40%). However, when synchronization occurs, the coupling strength was very low (only slightly above the significance threshold). In 40% of the experiments, when both PGN1 and PGN2 discharges were synchronized, the coupling ratios were different (at 0.76 Hz 1:1 and 2:1 and at 0.95 Hz 2:2 and 2:1 for PGN1 and PGN2 discharges respectively). In 40% of the experiments we found different types of dynamics in PGN discharges (i.e. n:m synchronization and aperiodicity in PGN1 and PGN2 discharges respectively).

5. Discussion

Since the analyses are usually based on visual inspection, the classification of the non linear interactions between a forcing event series and a forced one are limited by the low reproducibility of the results [2]. Visual inspection-based approaches become more and more impracticable in presence of noisy signals or sliding dynamics (i.e. the type of coupling patterns change during the recording). The proposed approach allows one to produce a classification virtually reducing to zero the human intervention through a sequence of rules that are easy to implement. In addition, the most repetitive pattern is extracted even in presence of noise or sliding dynamics.

The application to single postganglionic neurons discharges confirms the ability of the lung inflation cycle to synchronize sympathetic oscillators responsible for regulating single neurons activities [4]. Indeed, n:m periodic synchronized dynamics were found in 60% of the recordings. However, the interactions are very weak, as confirmed by the low values of the coupling strength. The analysis confirms also that sympathetic oscillators governing the single postganglionic neuron discharges work at different frequencies and/or behave differently

when forced by mechanical ventilation. Indeed, the discharges of the two neurons interact differently with ventilation (different types of dynamics are observed in 40% of the experiments) or, when both discharges are synchronized (it occurs in 40% of the experiments), the coupling ratios are different.

6. Conclusions

The proposed method is efficient in classifying the non linear interactions resulting from the driving action of an event series on a driven one and provides useful parameters such as the ratio and strength of the coupling. The method confirms that the lung inflation cycle is capable of synchronizing the discharges of single postganglionic neurons innervating the rat tail and that the underlying sympathetic oscillators form a population with different frequencies and/or different capabilities of synchronizing to the lung inflation cycle.

Acknowledgements

This study was supported by the Wellcome Trust.

References

- [1] Pikovsky A, Rosenblum M, Kurths J. Synchronization - An universal concept in non linear sciences. Cambridge University Press 2001.
- [2] Guevara MR, Shrier A, Glass L. Phase-locked rhythms in periodically stimulated heart cell aggregates. *Am J Physiol* 1988;254:H1-10.
- [3] Porta A, Montano N, Furlan R, Cogliati C, Guzzetti S, Gneccchi-Ruscione T, Malliani A, Chang H-S, Staras K, Gilbey MP. Automatic classification of interferences patterns in driven event series: application to single sympathetic neuron discharge forced by mechanical ventilation (submitted to *Biol Cybern*).
- [4] Chang H-S, Staras K, Gilbey MP. Multiple Oscillators provide metastability in rhythm generation. *J Neurosci* 2000;20:5135-43.
- [5] Porta A, Baselli G, Liberati D, Montano N, Cogliati C, Gneccchi-Ruscione T, Malliani A, Cerutti S. Measuring the degree of regularity by means of a corrected conditional entropy in sympathetic outflow. *Biol Cybern* 1998;78:71-78.
- [6] Theiler J, Eubank S, Longtin A, Galdrikian B, Farmer JD. Testing for nonlinearity in time series: the method of surrogate data. *Physica D* 1992;58:77-94.

Address for correspondence.

Alberto Porta, PhD
Universita' degli Studi di Milano
Dipartimento di Scienze Precliniche (DiSP)
LITA di Vialba
Via G.B. Grassi 74
20157, Milan
Italy

E-mail: alberto.porta@unimi.it